

First Place Solution to the MLCAS 2025 GWFSS Challenge: The Devil is in the Detail and Minority

Songliang Cao Tianqi Hu Hao Lu*

National Key Laboratory of Multispectral Information Intelligent Processing Technology

School of Artificial Intelligence and Automation

Huazhong University of Science and Technology, China

songliangcao@126.com hlu@hust.edu.cn

Abstract

In this report, we present our solution during the participation of the MLCAS 2025 GWFSS Challenge. This challenge hosts a semantic segmentation competition specific to wheat plants, which requires to segment three wheat organs including the head, leaf, and stem, and another background class. In 2025, participating a segmentation competition is significantly different from that in previous years where many tricks can play important roles. Nowadays most segmentation tricks have been well integrated into existing codebases such that our naive ViT-Adapter baseline has already achieved sufficiently good performance. Hence, we believe the key to stand out among other competitors is to focus on the problem nature of wheat per se. By probing visualizations, we identify the key—the stem matters. In contrast to heads and leaves, stems exhibit fine structure and occupy only few pixels, which suffers from fragile predictions and class imbalance. Building on our baseline, we present three technical improvements tailored to stems: i) incorporating a dynamic upsampler SAPA used to enhance detail delineation; ii) leveraging semi-supervised guided distillation with stem-aware sample selection to mine the treasure beneath unlabeled data; and iii) applying a test-time scaling strategy to zoom in and segment twice the image. Despite being simple, the three improvements bring us to the first place of the competition, outperforming the second place by clear margins. Code and models will be released at <https://github.com/tiny-smart/gwfss25>.

1. Introduction

The 7th International Workshop on Machine Learning for Cyber-Agricultural Systems (MLCAS 2025), in conjunction with the Computer Vision in Plant Phenotyping and

*corresponding author

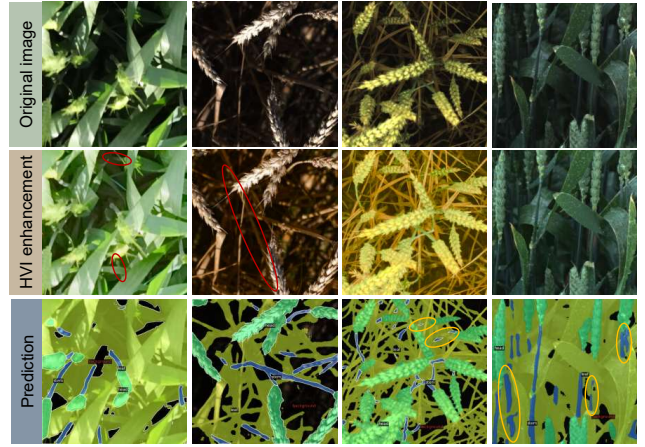


Figure 1. Visual inspection of the ViT-Adapter predictions on the GWFSS validation set. Our intuition tell us that the performance bottleneck seems to lie in the stem class, which not only requires good detail delineation but also needs to tackle the minority of pixel occupancy. Images in the second row are enhanced by the HVI color space [19] for ease of interpretation. The red circle seems to be stems segmented missed and the yellow one seems to be stems segmented roughly.

Agriculture (CVPPA) workshop at International Conference on Computer Vision (ICCV 2025), host a competition called Global Wheat Full Semantic Segmentation (GWFSS). The competition aims to advance pixel-level understanding of wheat plants, i.e., segmenting the full plant components, including four classes of leaf, stem, head, and background, to comprehensively describe plant architecture, health, and development. In this report, we present our winner solution to this competition.

The competition has two phases. In the development phase (Phase 1), participants can have access to a small subset of fully labeled training data (only 99 samples) and a large amount of unlabeled data (64,368 samples); validation data (only images) are provided for participants to build

and iterate their models. In the testing phase (Phase 2), the top 20 participants are invited to generate inference results on the test set using the final model from Phase 1. Different from other unconstrained open challenges, there are three rules in this competition: i) only ImageNet-1K pre-trained backbones are allowed to use; ii) only the provided GWFSS training data is allowed to use, and participants cannot use other unlabeled datasets for pre-training; iii) manual labeling or annotation is strictly prohibited.

To quickly gain a first impression of the visual challenges of this task, we trained a state-of-the-art ViT-Adapter with the Mask2Former head using the labeled training data. Some visualizations on the validation set are shown in the Fig. 1. Due the significant illumination variations, we resort to a recent learnable HVI color space [19] for ease of interpretation of segmentation results. This color space significantly enhances the contrast of low-light regions such as shadows and reveals many missing details. According to Fig. 1, we have the following observations and insights.

Remark 1. *The fine structure of the stem class leads to difficult boundary predictions such that the model needs to enhance detail awareness.*

By observing the patterns of visualization results, we find that the `head`, `leaf`, and `background` classes are well segmented in general, while the `stem` class exhibits a high degree of fragile predictions. We therefore test the class IoU metric on the training dataset with available ground truths: the `stem` class only reports 0.69 mIoU, while the other three classes achieve 0.88, 0.91, and 0.90 for `background`, `head`, and `leaf`, respectively. It seems that the performance bottleneck lies in the `stem` class. In our view, we believe an effective way to alleviate this bottleneck is to enhance detail awareness of the model. Technically, this amounts to the question on how to improve the quality of high-resolution feature maps.

Remark 2. *The model may risk overfitting due to rather limited labeled data such that unlabeled data should be exploited.*

The labeled training data are limited (only 99 images are provided), but our baseline model has more than 200M parameters, which makes it prone to overfitting. Therefore, how to effectively leveraging the unlabeled data seems to be another key to improve model generalization. In open literature, there are two mainstream ways to exploit the unlabeled data: i) resorting to self-supervised learning to pre-train a vision backbone (e.g., MAE [7] and DINOv2 [15]); ii) leveraging semi-supervised learning to learn a robust model (e.g. Mean Teacher [16]). We will choose one of the two routes.

Remark 3. *The stem class only occupies a small number of pixels such that the model may suffer from class imbalance.*

By analyzing the number of pixel labels of each class in the training dataset, we find that the proportions of `background`, `head`, `stem`, and `leaf` pixels are 85 : 27 : 9 : 137, respectively. It seems *the devil is in the detail and minority*: the `stem` class is not only subtle to segment but also underrepresented in the dataset. Hence, we believe we also need to address the class imbalance issue and increase the visibility of the `stem` class during model training.

To address the challenges above, we build upon a state-of-the-art segmentation framework ViT-Adapter [3] and present three technical improvements. Considering that detail delineation is closely related to the quality of high-resolution feature maps, we first incorporate a dynamic upsampling operator SAPA [13] into the Mask2Former head [4] to enhance the detail delineation of the model. Second, we apply a semi-supervised learning pipeline with guided distillation [2] to leverage the unlabeled training set. Note that, to alleviate the class imbalance and increase the exposure of the `stem` class, we do not use the entire unlabeled data but carefully choose a small portion of stem-related image data to form a subset (4500 images), filtered by a model trained with labeled training data. Finally, we conduct a form of test-time scaling with a *zoom in and segment twice* strategy, which zooms in images to different scales and segment the image of each scale following a sliding-window style inference. This strategy significantly benefits the prediction of the `stem` class. Combining the three improvements, our final solution achieves the first place in the competition during both the development phase and the testing phase, reporting 0.77 and 0.75 mIoU metric, respectively, outperforming the second place by clear margins. While the three improvements seem simple, we hope our solution can inform the plant phenotyping community that a simple tweak can make a difference if one identifies the bottleneck correctly.

2. GWFSS Competition Dataset

The competition is based on the GWFSS dataset. The GWFSS dataset is a Siamese dataset to the Global Wheat Head Detection (GWHD) dataset [5]. Unlike the GWHD dataset focusing on an object detection task, the GWFSS dataset highlights pixel-wise understanding, that is, semantic segmentation, of plant organs including the `head`, `stem`, and `leaf`, aiming to comprehensively describe the architecture, health, and development of wheat plants.

Similar to the GWHD dataset, the GWFSS dataset is built with international support, with 11 institutes and universities from diverse geographical regions using various imaging setups. Such a diversity ensures that the dataset covers sufficiently large variations in environmental conditions, genotypes, and illumination, which results in visual challenges such as appearance changes, shadows, and complex background. Even the wheat plants within the same do-



Figure 2. **Samples of different domains in the GWFSS dataset.** Domain 1-9 are used for training and validation, and domain 0 is used for testing. Different domains exhibit significant intrinsic and extrinsic variations.

main can encompass multiple growth stages, leading to intrinsic morphological variations. As shown in Fig. 2, there is a substantial distribution gap between images from different domains. This renders significant difficulties in building a robust segmentation. In particular, the GWFSS dataset is split into a training set, a validation set, and a testing set. The training data and validation data are both selected from 9 out of 10 domains, where the labeled training data and the validation data have 99 images, and the unlabeled training data are more than 60,000. The left domain, with 110 images, is used for testing data to test the generalization of the model. The data splits are summarized in Table 1. All images in the dataset have a resolution of 512×512 . Only the ground truths of the labeled training data are provided. To test on the validation data and testing data, participants must submit their results to the `codabench` online platform.¹

3. Proposed Solution

Recently some vision foundation models such as DINOv2 [15] have emerged and demonstrated robust performance across a range of downstream tasks. Indeed many top-performing solutions in open challenges are built upon fine-tuning large vision models. However, since the competition only allows to use ImageNet-1K pretrained backbones, we turn our focus to the problem nature of the task and mainly address the challenges we observe above. The overview of our solution is shown in Fig. 3. Our solution includes three stages: training a supervised segmentation baseline, applying a semi-supervised semantic segmentation pipeline, and leveraging a sliding-window-style test-time scaling strategy.

3.1. SAPA-Enhanced ViT-Adapter

We choose the ViT-Adapter [3] as our baseline, because current state-of-the-art semantic segmentation models are typically based on the architecture of vision trans-

data splits	training		validation	testing
	labeled	unlabeled		
#Images	99	64,368	99	110

Table 1. **Training, validation, the testing splits of the GWFSS competition dataset.**

former (ViT) [6]. In particular, we adopt the BEiT_{v2} and ImageNet-1K pretrained ViT-Large model.² By feeding the input image tokens into the ViT-Adapter, multi-scale features $\{\mathcal{F}_1^{\frac{1}{4}}, \mathcal{F}_2^{\frac{1}{8}}, \mathcal{F}_3^{\frac{1}{16}}, \mathcal{F}_4^{\frac{1}{32}}\}$ are extracted, followed by the Mask2Former head [7]. In the pixel decoder of Mask2Former, the three low-resolution features $\{\mathcal{F}_2^{\frac{1}{8}}, \mathcal{F}_3^{\frac{1}{16}}, \mathcal{F}_4^{\frac{1}{32}}\}$ are refined through several layers of multi-scale deformable attention [18], and the output are denoted by $\{\mathcal{O}_2^{\frac{1}{8}}, \mathcal{O}_3^{\frac{1}{16}}, \mathcal{O}_4^{\frac{1}{32}}\}$. The decoder feature $\mathcal{O}_2^{\frac{1}{8}}$ is upsampled and fused with $\mathcal{F}_1^{\frac{1}{4}}$ to obtain the mask feature $\mathcal{F}_{\text{mask}}$, and $\mathcal{F}_{\text{mask}}$ is jointly used with the mask query embedding $\mathcal{Q}_{\text{mask}}$ to predict final segmentation mask M as

$$M = g(\mathcal{Q}_{\text{mask}}, \mathcal{F}_{\text{mask}}), \quad (1)$$

where $g(\cdot)$ is the mask predictor. Eq. (1) indicates that the quality of $\mathcal{F}_{\text{mask}}$ is closely related to the quality of the final predicted masks M .

Recall that our goal is to enhance the prediction of the `stem` class. The fine structure of the stem requires the model to have clear detail delineation in the high-resolution mask feature $\mathcal{F}_{\text{mask}}$. According to open literature [9–14], one critical stage that affects the quality of $\mathcal{F}_{\text{mask}}$ is feature upsampling. Unfortunately, the standard Mask2Former head uses bilinear interpolation for upsampling, which would *ipso facto* blur details. Hence, we propose to replace bilinear upsampling with SAPA [13] to enhance the detail awareness of the model.

SAPA enhances detail delineation by modeling the mutual similarity between the low-resolution decoder neighborhood and the high-resolution encoder feature point in the upsampling kernel. Formally, given a local decoder neighborhood \mathcal{N}_l informed by the location l , the corresponding upsampling weight w_l takes the form

$$w_l = \frac{h(\text{sim}(x, y))}{\sum_{z \in \mathcal{N}_l} h(\text{sim}(z, y))}, \quad (2)$$

where x is the decoder feature point, y the encoder feature point, $\text{sim}(\cdot, \cdot)$ the similarity function, and $h(\cdot)$ the normalization function. It has been proved that such a formulation has conditional boundary sharpness and conditional

¹<https://www.codabench.org/competitions/5905/>

²https://github.com/microsoft/unilm/blob/master/beit2/get_started_for_image_classification.md

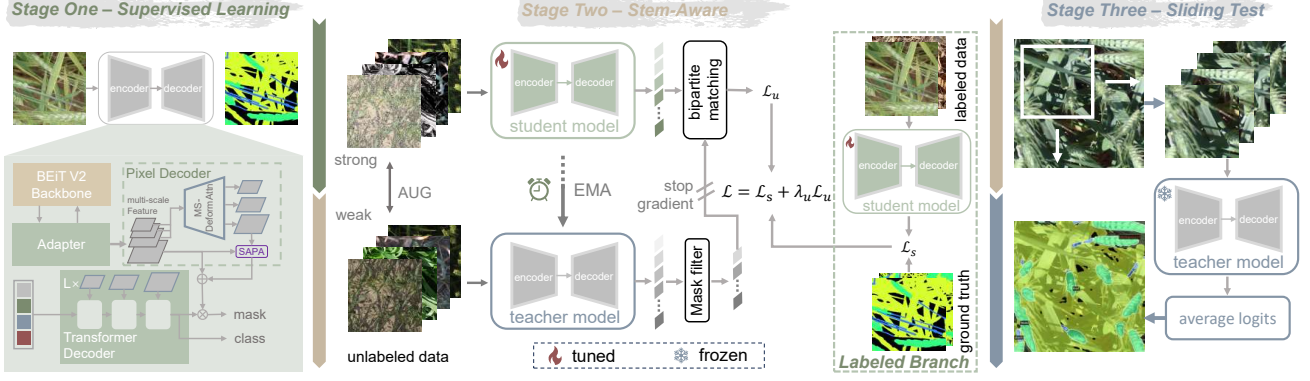


Figure 3. **The overview of our solution.** Our solution includes three stages: in stage one, we leverage the labeled training dataset to train a supervised baseline ViT-Adapter and enhance its detail delineation with a dynamic upsampler SAPA; in stage two, we apply a semi-supervised learning pipeline with guided distillation on both labeled data and selected unlabeled data; in stage three, we implement a form of test-time scaling by zooming in images and segmenting twice following the sliding-window-style inference.

smoothness guarantees [13]. We choose the similarity function to be gated similarity $\text{sim}(x, y) = gx^T Py + (1 - g)x^T Qy$, where $g \in (0, 1)$ is a gating unit learned by linear projection, and P and Q are learnable projection matrices. $h(\cdot)$ is chosen to be the softmax normalization. In this way, Eq. (2) computes the bilinear kernel [17]. With SAPA, the mask feature $\mathcal{F}_{\text{mask}}$ amounts to

$$\mathcal{F}_{\text{mask}} = \mathcal{F}_1^{\frac{1}{4}} + \text{SAPA}(\mathcal{F}_1^{\frac{1}{4}}, \mathcal{O}_1^{\frac{1}{8}}). \quad (3)$$

The effect of SAPA can refer to Fig. 4. It can be observed that SAPA effectively enhances detail delineation and reduces fragile mask predictions.

3.2. Guided Distillation with Stem-Aware Sample Selection

As aforementioned, one can choose two routes, *i.e.*, self-supervised pretraining or semi-supervised learning, to exploit the unlabeled data provided by the competition. We finally choose the second route of semi-supervised learning. The reason is that, although there are over 60,000 unlabeled images, which is significantly more than the 99 labeled data, such a data scale may still be insufficient for self-supervised learning to train a robust vision backbone (DINOv2 uses 142M images [15]). Meanwhile, even with a well-pretrained backbone, fine-tuning is still required.

Mainstream semi-supervised learning is typically based on the Mean Teacher framework [16]. In this framework, there is often a Siamese network with two identical model architectures and parameters, where a teacher model generates soft predictions to guide the training of a student model. The teacher model is updated following the exponential moving average (EMA) with the parameters of the student model. Let θ_t^i and θ_s^i denote the weights of the

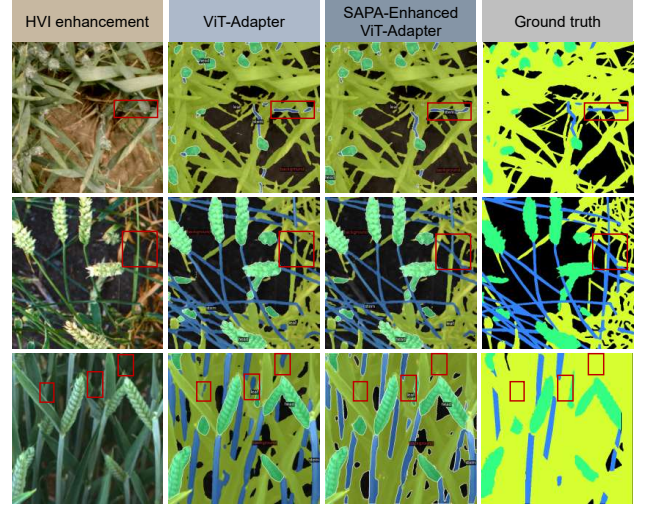


Figure 4. **Comparison between the naive ViT-Adapter baseline and SAPA-Enhanced ViT-Adapter.** The red rectangles indicate that SAPA-Enhanced ViT-Adapter is more effective than the vanilla ViT-Adapter in tackling the segmentation of stem structures, with less misclassifications and missing segmentations.

teacher model and the student model at the i -th iteration, respectively. The teacher model is updated as

$$\theta_t^{i+1} = \alpha \theta_t^i + (1 - \alpha) \theta_s^{i+1}, \quad (4)$$

where α is a damping factor. For each unlabeled sample, the teacher and student models receive perturbed versions of the same input (e.g., different augmentations), and the student is trained to match the output of the teacher model, encouraging consistency between them. The meta pipeline of mean teacher enables the teacher model to learn from a large amount of unlabeled data and therefore enhances its

generalization ability.

In this competition, we adopt an improved guided distillation framework [2]. The overview of guided distillation is shown in the stage two of Fig. 3. Most existing distillation-based pipelines train a model on the labeled data as the student. However, this strategy can be suboptimal in our competition due to the fact that the student model may overfit the labeled training data (only 99 images). To address this, guided distillation introduces a guided burn-in stage, where the student model is allowed to learn from both labeled and unlabeled data. Before guided distillation, the teacher model is first trained on the labeled data and is used to generate pseudo labels for the student model (the stage one). Then the student model is initialized randomly and learned from both labeled and pseudo-labeled data. After the guided burn-in stage, the student model will transfer its weights to the teacher model and perform the standard EMA update.

To better adapt this framework to our problem, we further repurpose the idea of importance sampling [8] by selecting stem-aware samples from the unlabeled data. In particular, considering that the unlabeled data are organized into 9 domains, we select the top 500 samples with the most proportion of stem pixels in each domain conditioned on the pseudo-labeled masks, resulting in 4500 images in total. The stem-aware sample selection can maximize the presence of the stem class to the model, which somehow mitigates the problem of class imbalance.

The loss functions used follow the Mask2Former [7]. Given a wheat image x_i and its ground-truth segmentation mask $y_i = \{(y_i^k, c_i^k)\}_{k \in [1, n]}$ encoded by binary masks y_i^k 's and class indices c_i^k 's. For each sample, the model predicts K candidate masks $\{(\hat{y}_i^k, \hat{c}_i^k)\}_{1 \leq k \leq K}$. After bipartite matching, a matching (k, m_k) is obtained between the predictions and ground truths, where m_k is the index of the predicted mask matched to the k -th ground truth mask. The single-sample supervised loss \mathcal{L}_s^i thus can be defined by

$$\mathcal{L}_s^i = \frac{1}{n} \sum_{k=1}^n \ell_{ce}(\hat{y}_i^{m_k}, y_i^k) + \lambda_{dice} \ell_{dice}(\hat{y}_i^{m_k}, y_i^k) + \lambda_c \ell_c(\hat{y}_i^{m_k}, y_i^k), \quad (5)$$

where ℓ_{ce} is the cross-entropy loss, ℓ_{dice} is the dice loss, ℓ_c is the binary cross-entropy, and λ_{dice} and λ_c are hyperparameters used to control the contribution of different losses. The unsupervised loss \mathcal{L}_u w.r.t. the unlabeled data is identical to the supervised one \mathcal{L}_s , except that the ground truth labels are replaced by the pseudo masks generated from the teacher model. By removing the superscript i for \mathcal{L}_s^i , the final guided distillation takes the form

$$\mathcal{L} = \mathcal{L}_s + \lambda_u \mathcal{L}_u, \quad (6)$$

where λ_u weights the importance of the unsupervised loss.

Note that, guided distillation only uses 99 labeled images and the selected 4500 unlabeled images.

3.3. Zoom In and Segment Twice

Small- and fine-object visual perception has been long-standing hard cases for semantic segmentation. In our case, the `stem` class is identified to be the bottleneck due to its not only small-proportion but also fine-structure characteristics. After the stage-two training, we have achieved fairly good performance on the leaderboard, but not competitive enough to secure the first place. Hence, in the rest time of the competition, we start to seek other training-free solutions to improve the performance of the `stem` class further. Inspired by slicing-aided hyper inference [1] which has shown strong performance in detecting small objects, we adapt this idea to wheat segmentation and develop a test-time scaling strategy called *zoom in and segment twice*. This strategy is initially inspired by an surprising observation that a significant performance improvement can be achieved by simply testing on a zoomed-in version of image. By scaling the image resolution from 512×512 to 768×768 , the performance improves from 0.74 to 0.76, which suggests the `stem` class can benefit from high-resolution inference.

Formally, given a scaling ratio $\sigma \geq 1$, we define a ZoomIn operator such that $I^\sigma = \text{ZoomIn}(I, \sigma)$, which zooms in the input image I from its original size (H, W) to I^σ a larger size $(\sigma H, \sigma W)$. During inference, given a sliding window size $k = (k_h \times k_w)$ with a stride $t = (t_h, t_w)$, where the subscript h and w indicate the height and width components, we further define a Slide operator such that $\{I_{i,j}^\sigma\} = \text{Slide}(I^\sigma, k, t)$, which slides the image I^σ , crop it into sub-window $\{I_{i,j}^\sigma\}$, where $\{I_{i,j}^\sigma\} = \{I^\sigma[i : i + k_h, j : j + k_w] \mid i = 0, t_h, \dots, \sigma H - k_h; j = 0, t_w, \dots, \sigma W - k_w\}$.

For each sliding window, we have the prediction logit for each window $L_{i,j}^\sigma = \text{Infer}(I_{i,j}^\sigma)$, where `Infer` means the model inference process. We then apply zero padding to match each logit to the original input resolution and average all the logits. During logit averaging, a count map $C \in \mathbb{R}^{\sigma H \times \sigma W}$ is recorded to indicate the number of times each pixel covered by the sliding windows. The final aggregated logit L^s is obtained by dividing the summed logits by the count map as

$$L^s = \frac{1}{C} \cdot \sum \text{Pad}(\text{Infer}(\text{Slide}(\text{ZoomIn}(I, \sigma)), k, t)), \quad (7)$$

where `Pad`(\cdot) is the zero padding operator.

The ‘zoom in’ strategy can be easily extended to multi-scale scenarios, which implements the ‘segment twice’ idea. Given a set of multi-scale ratio $S = \{\sigma_0, \sigma_1, \dots, \sigma_n\}$. For each ratio, we apply the same single-scale inference process above to obtain L^{σ_i} . Then, we can simply average the pre-

Method	SAPA	guided distillation	test time scaling	mIoU
baseline				0.7284
	✓			0.7291
	✓	✓		0.7432
	✓	✓	✓	0.7704

Table 2. **Ablation of different stages during the development phase.**

dicted logits across different scales to obtain the final logits

$$L = \frac{\sum_{\sigma_i \in S} \text{DownSample}(L^{\sigma_i}, \sigma_i)}{|S|}, \quad (8)$$

where $\text{DownSample}(\cdot, \sigma)$ means downsampling the input with the ratio σ .

4. Results and Discussions

Here we present our results and discussions. Before that, we first introduce the evaluation metric used and our implementation details.

4.1. Evaluation Metric

The evaluation metric follows the standard semantic segmentation metric, that is, the mean Intersection over Union (mIoU), which is defined by

$$\text{mIoU} = \frac{1}{N} \sum_{i=0}^N \frac{\text{TP}_i}{\text{TP}_i + \text{FP}_i + \text{FN}_i}, \quad (9)$$

where N is the number of classes. TP, FP, and FN denote the number of true positives, false positives, and false negatives for each class, respectively.

4.2. Implementation Details

We use the ImageNet-1K pretrained weight of BEiT_{v2}-Large from the official repository, which has first trained for 1600 epochs in a self-supervised manner and then fine-tuned for another 50 epochs following supervised learning. During our supervised learning stage for training a segmentation model, the model is trained for 20K iterations, with a batch size of 16. The base learning rate is set to 0.0001, and the backbone learning rate is 0.01. We use the play LRScheduler and set the warm up iterations to 0. The first stage takes approximately 5 hours to complete. In the guided distillation stage, we set the total iterations to 90K, with 20K iterations for guided burn-in stage and apply early stop strategy. This stage requires about three days of training time. For the loss weights, we set $\lambda_{\text{dice}} = 5$, $\lambda_c = 5$, and $\lambda_u = 2$. The EMA decay rate α is set to 0.9996. In the testing stage, we use scaling ratios

Testing Scale	Leaderboard Score
512	0.74
768	0.76
512, 768, 1024, 1280, 1536, 1792	0.77

Table 3. **Scores with different test-time scaling configurations.** Through the strategy of *zoom in and segment twice*, we achieved a significant improvement. While extend our strategy to multi-scales, we can improve the performance further.

Team Name	Development Phase	Testing Phase
HUST_TinySmart (Ours)	0.77	0.75
ZR Yang&JH Jiang	0.75	0.71
good	0.75	-
tapu1996	0.74	n/a
pcccl	0.74	0.7
willer	0.74	-
asuka	0.74	0.69
nccckuu	-	0.68
enchanter	0.71	0.66
zaorui_njfu	0.71	0.65
Dafang Zou	0.71	-
tiezhuma	0.7	0.64
phasheen	0.69	-
jaykk	0.69	-
xmba15	0.69	0.63
dsvolkov	0.66	0.62
zengyangche	0.67	0.61
perrychen	0.64	-
HZAU AISLE Group	0.63	0.57
loannis Droutsas	0.57	0.54

Table 4. **Official leaderboard scores.** Top 20 teams from the development phase only (as of June 21, 2025). The scores are rounded mIoU.

$\S = \{1.0, 1.5, 2.0, 2.5, 3.0, 3.5\}$ to scale the input image and apply sliding inference for each image. All experiments are conducted on the Ubuntu 20.04 system and on a workstation with four 48 GB RTX A6000 GPUs, two 10-core Intel Xeon Silver 4210R CPUs, and 256 GB RAM.

4.3. Main Results

The effect of our different stages in the development phase can be found in Table 2. Results justify that each our design choice makes a difference. Surprisingly, the test time scaling stage yields the most significant improvement, improving the stage-two model by 0.0272 scores. A plausible explanation is that the model can better sense the detail of the stem class when zooming in the image. We also test the effect of different scaling ratios. The scores can be found in Table 3. It can be observed that the single-scale zoom-in operation brings the most significant improvement. While our final solution uses the multi-scale inference strategy (segment twice), it introduces significant computational cost.

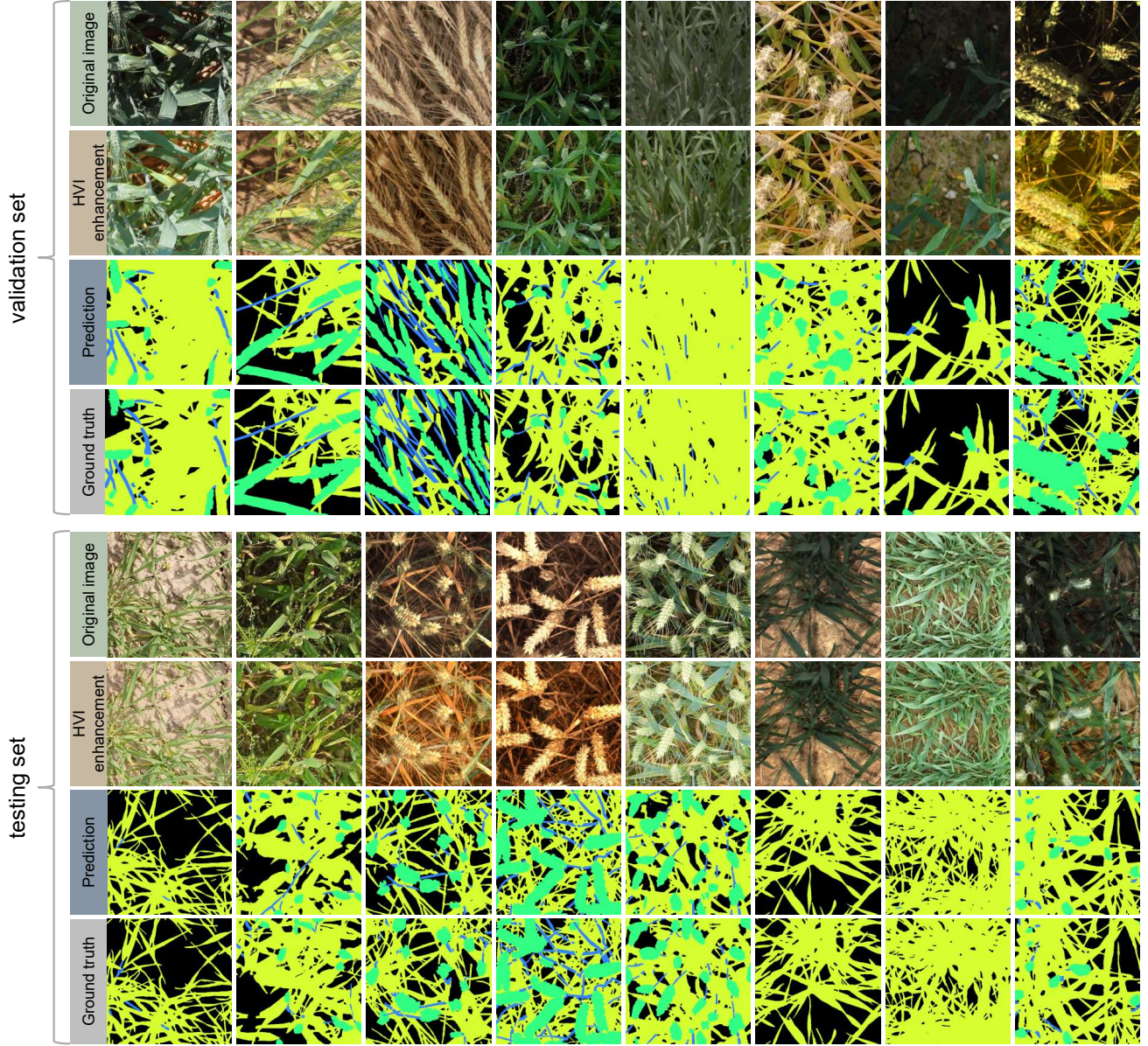


Figure 5. Visualization of our model on validation and testing set.

The final competition results of the development and testing phases are shown in Table 4. Through our three improvements, we finally achieve a score of 0.7704 in the development phase and 0.7468 in the testing phase. Our solution ranks the first place on both the development and testing leaderboard. Remarkably, it exhibits the least performance drop in the testing phase, indicating strong generalization of our solution. In our view, this is mainly attributed to guided distillation, which enhances the training robustness of the model. Although our three improvements seem to be simple, we believe the key to our success is to follow the philosophy of the devil is in the detail and minority, that

is, the `stem` class. The qualitative results of our final model are shown in Fig. 5.

5. Conclusion

This report presents our first place solution to the MLCAS 2025 GWFSS Challenge. Due to the significant illumination variations, we resort to the HVI color space for ease of analysis of segmentation results. Our approach is based on three insights observed from our baseline. By integrating the SAPA dynamic upsampling module into the ViT-Adapter, the ability of the model to capture fine details and

tackle object boundaries is enhanced. Through guided distillation, we effectively leverage the unlabeled data, leading to improved model performance and enhanced robustness. Finally, through the strategy of *zoom in and segment twice*, we further improve the performance of the model during the test time. We hope our solution can provide insights to future studies, especially on how to identify the bottleneck of the problem.

Acknowledgement

This work is jointly supported by the Hubei Provincial Natural Science Foundation of China under Grant No. 2024AFB566 and by the HUST Undergraduate Natural Science Foundation under Grant No. 62500034.

References

- [1] Fatih Cagatay Akyon, Sinan Onur Altinuc, and Alptekin Temizel. Slicing aided hyper inference and fine-tuning for small object detection. In *Proceedings of IEEE International Conference on Image Processing*, pages 966–970. IEEE, 2022. 5
- [2] Tariq Berrada, Camille Couprie, Karteek Alahari, and Jakob Verbeek. Guided distillation for semi-supervised instance segmentation. In *Proceedings of the IEEE/CVF Winter Conference on Applications of Computer Vision*, pages 475–483, 2024. 2, 5
- [3] Zhe Chen, Yuchen Duan, Wenhai Wang, Junjun He, Tong Lu, Jifeng Dai, and Yu Qiao. Vision transformer adapter for dense predictions. In *Int. Conf. Learn. Represent.*, 2023. 2, 3
- [4] Bowen Cheng, Ishan Misra, Alexander G Schwing, Alexander Kirillov, and Rohit Girdhar. Masked-attention mask transformer for universal image segmentation. In *Proceedings of the IEEE/CVF Conference on Computer Vision and Pattern Recognition (CVPR)*, pages 1290–1299, 2022. 2
- [5] Etienne David, Simon Madec, Pouria Sadeghi-Tehran, Helge Aasen, Bangyou Zheng, Shouyang Liu, Norbert Kirchgessner, Goro Ishikawa, Koichi Nagasawa, Minhajul A Badhon, et al. Global wheat head detection (gwhd) dataset: A large and diverse dataset of high-resolution rgb-labelled images to develop and benchmark wheat head detection methods. *Plant Phenomics*, 2020. 2
- [6] Alexey Dosovitskiy, Lucas Beyer, Alexander Kolesnikov, Dirk Weissenborn, Xiaohua Zhai, Thomas Unterthiner, Mostafa Dehghani, Matthias Minderer, Georg Heigold, Sylvain Gelly, et al. An image is worth 16x16 words: Transformers for image recognition at scale. In *Int. Conf. Learn. Represent.*, 2021. 3
- [7] Kaiming He, Xinlei Chen, Saining Xie, Yanghao Li, Piotr Dollár, and Ross Girshick. Masked autoencoders are scalable vision learners. In *Proceedings of the IEEE/CVF Conference on Computer Vision and Pattern Recognition (CVPR)*, pages 16000–16009, 2022. 2, 3, 5
- [8] Alexander Kirillov, Yuxin Wu, Kaiming He, and Ross Girshick. PointRend: Image segmentation as rendering. In *Proceedings of the IEEE/CVF Conference on Computer Vision and Pattern Recognition (CVPR)*, pages 9799–9808, 2020. 5
- [9] Wenze Liu, Hao Lu, Hongtao Fu, and Zhiguo Cao. Learning to upsample by learning to sample. In *Proceedings of the IEEE/CVF International Conference on Computer Vision*, pages 6027–6037, 2023. 3
- [10] Hao Lu, Yutong Dai, Chunhua Shen, and Songcen Xu. Indices matter: Learning to index for deep image matting. In *Proceedings of the IEEE/CVF International Conference on Computer Vision*, pages 3266–3275, 2019.
- [11] Hao Lu, Yutong Dai, Chunhua Shen, and Songcen Xu. Index networks. *IEEE Transactions on Pattern Analysis and Machine Intelligence*, 44(1):242–255, 2022.
- [12] Hao Lu, Wenze Liu, Hongtao Fu, and Zhiguo Cao. Fade: Fusing the assets of decoder and encoder for task-agnostic upsampling. In *European Conference on Computer Vision*, pages 231–247, 2022.
- [13] Hao Lu, Wenze Liu, Zixuan Ye, Hongtao Fu, Yuliang Liu, and Zhiguo Cao. Sapa: Similarity-aware point affiliation for feature upsampling. In *Advances in Neural Information Processing Systems (NeurIPS)*, pages 20889–20901, 2022. 2, 3, 4
- [14] Hao Lu, Wenze Liu, Hongtao Fu, and Zhiguo Cao. Fade: A task-agnostic upsampling operator for encoder–decoder architectures. *International Journal of Computer Vision*, 133(1):151–172, 2025. 3
- [15] Maxime Oquab, Timothée Darcet, Théo Moutakanni, Huy Vo, Marc Szafraniec, Vasil Khalidov, Pierre Fernandez, Daniel Haziza, Francisco Massa, Alaaeldin El-Nouby, et al. DINOv2: Learning robust visual features without supervision. *arXiv preprint arXiv:2304.07193*, 2023. 2, 3, 4
- [16] Antti Tarvainen and Harri Valpola. Mean teachers are better role models: Weight-averaged consistency targets improve semi-supervised deep learning results. *Advances in Neural Information Processing Systems (NeurIPS)*, 30, 2017. 2, 4
- [17] Joshua B Tenenbaum and William T Freeman. Separating style and content with bilinear models. *Neural Computation*, 12(6):1247–1283, 2000. 4
- [18] Zhuofan Xia, Xuran Pan, Shiji Song, Li Erran Li, and Gao Huang. Vision transformer with deformable attention. In *Proceedings of the IEEE/CVF Conference on Computer Vision and Pattern Recognition (CVPR)*, pages 4794–4803, 2022. 3
- [19] Qingsen Yan, Yixu Feng, Cheng Zhang, Guansong Pang, Kangbiao Shi, Peng Wu, Wei Dong, Jinqiu Sun, and Yanling Zhang. HVI: A new color space for low-light image enhancement. In *Proceedings of the IEEE/CVF Conference on Computer Vision and Pattern Recognition (CVPR)*, pages 5678–5687, 2025. 1, 2